Article ID: 1000-324X(2016)12-1370-05 **DOI:** 10.15541/jim20160152

Optical and Structural Properties of Carbon Nanotubes/Black Nickel Composite Coatings by Electrodeposition

ZOU Si-Hao, XIN Shi-Gang, SONG Li-Xin

(Key Laboratory of Inorganic Coating Materials, Shanghai Institute of Ceramics, Chinese Academy of Sciences, Shanghai 200050, China)

Abstract: Carbon nanotubes/black nickel composite coatings with high optical properties on titanium alloy substrate were prepared on the basis of composite electrochemical deposition methods. Micro scale morphology and optical properties of as-prepared materials were analyzed. The effects of carbon nanotubes concentration and electroplating current density on the optical properties were also explored. The results show that grain size of composite coating was small with microporous and increased surface roughness as compared with conventional black nickel coating. The absorptance (α_s) over a spectral range of 300–2300 nm was up to 98%, while the emittance (ε) over a 2.5 μm to 20 μm range was 94%, better than those of conventional black nickel coatings. The absorptance of composite coating increased firstly and then decreased with increase of carbon nanotubes concentration and electroplating current density.

Key words: carbon nanotube; electrodeposition; composite coating; solar absorptance

Highly-efficient light absorption materials are of great significance for multiple applications in optical instruments[1-2], absorption materials[3], aerospace, and defense industries[4]. Light absorption materials can be obtained through chemical treatment[5], plating[6] and painting[7]. Black nickel consisting of nickel, zinc, nickel- and zinc-sulphide[8], which is prepared by electrodeposition method, shows distinctive properties for optical instruments[9]. Optical characteristics of black materials should be close to a black body[10]. Currently, however, the optical properties of black nickel coating do not match this requirement. Since carbon nanotube (CNT) was discovered in 1991[11], it has attracted tremendous interests from numerous scientists because of its mechanical, thermal, electronic, and optical properties[12-13]. As for the optical property, one-dimensional structure of CNTs possesses special bandgap which lead to strong optical absorption over a broad band[14]. The film of multi-walled carbon nanotubes (MWCNTs) can absorb the incident light involving spectrum from ultraviolet to infrared region[15].

Recently, it has been found that some coatings fabricated using CNT forests can give ultra-low reflection and high absorption[16-17]. Such unique optical property of CNT endows it ideal material for optic devices[18]. Actually, the morphology and structure of CNTs can be maintained when CNTs are doped into other materials[19]. Therefore, CNT is regarded as an ideal additive of composite materials. However, rare studies have been made to promote the optical properties so far by introducing MWCNTs into black nickel coatings.

This paper reported a novel CNTs/black nickel composite coating with excellent optical properties which were fabricated by using the electrochemical deposition method.

1 Experimental

The effective utilization of CNTs in composite applications depends on dispersing the CNTs homogeneously through the matrix[20]. Moreover, CNTs functionalized with carboxylic groups were used to improve the dispersion of CNTs in solution. The carboxylic MWCNTs were purchased from Nanjing XFNANO Materials Tech Co., Ltd. To be specific, the outside diameter, length and carboxyl compound of CNTs are 10–20 nm, 0.5–2 μm and 2%, respectively (Fig. 1). Their diameter and length coincide with the mentioned by supplier. Sodium dodecylsulfate (SDS) was used as dispersing agent to disperse MWCNTs in the black nickel electrolyte with ultrasonic agitation method for 2 h.

Received date: 2016-03-15; **Modified date:** 2016-05-18
Biography: ZOU Si-Hao (1990–), male, candidate of Master degree. E-mail: zousihao@student.sic.ac.cn
Corresponding author: XIN Shi-Gang, professor. E-mail: sgxin@mail.sic.ac.cn

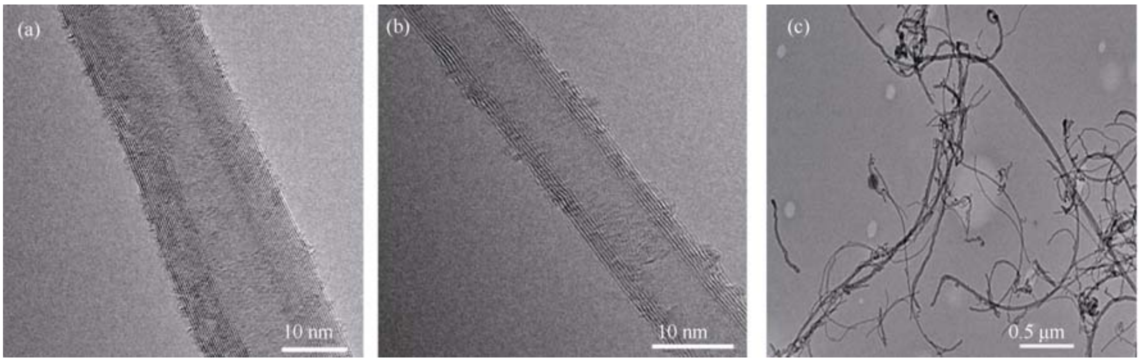

Fig. 1　TEM images of carbon nanotubes (a, b, c)

The electrodeposition of black nickel was carried out using a bath containing analytical grade: $NiSO_4{\cdot}6H_2O$ 90 g/L, $ZnSO_4{\cdot}7H_2O$ 50 g/L, Ni $(NH_4)_2(SO_4)_2{\cdot}6H_2O$ 55 g/L and NaSCN 30 g/L. The concentration of MWCNTs and SDS is 0.5–1.5 g/L and 0.75–1.5 g/L, respectively. For electrodeposition, a titanium alloy sheet of dimension 20 mm×20 mm×1 mm was used as cathode. Also, a graphite sheet of dimension 100 mm×72 mm×5 mm was used as anode. Previous to the electrodeposition procedure, the titanium alloy substrate was washed with oil, acid and alkali solution to avoid contamination. A current density of 0.3–0.6 A/dm^2 was applied, and the deposition time was 60 min in the process of electrodeposition. In addition, the bath temperature was controlled in the range of 25–35℃ and the pH of the electrolyte was maintained at 4.6–6.2.

The morphology of coated samples has been investigated by a scanning electoral microscope (SEM Hitachi S3400 & SU8820). Additionally, the optical measurement in the wavelength range (0.3–2.3 μm) was recorded using a UV/VIS/NIR spectrometer (Perkin Elmer Lambda 950) equipped with an integrating sphere. As for infrared reflection measurement, the near-normal reflectance in the wavelength range of 2.5–20 μm was measured by FT-IR spectrometer (Bruker Equinox 55) equipped with directional reflectometer accessory.

For an opaque object, the spectral absorptivity (α_λ) is equal to $1-\rho_\lambda$ (ρ_λ is the spectral reflectivity), The solar absorptance, α_s, is defined as a weighted fraction of the absorbed radiation to the incoming solar radiation on a surface[21]. Thus, the solar absorptance α_s could be calculated using following formula

$$\alpha_s = \frac{\int_{\lambda_1}^{\lambda_2} I_{sol}(\lambda)(1-p_\lambda)\,d\lambda}{\int_{\lambda_1}^{\lambda_2} I_{sol}(\lambda)\,d\lambda} \tag{1}$$

Where I_{sol} signifies the spectral solar irradiance which is defined in accordance with ISO standard 9845-1(1992) for air mass of 1.5. λ denotes the wavelength of incident light and ρ_λ signifies the reflectance at a certain wavelength. According to Kirchhoff's law, the spectral emissivity (ε_λ) equals to the spectral absorptivity (α_λ) at the thermal equilibrium condition. Hence, the spectral emissivity (ε_λ) is equal to $1-\rho_\lambda$(ρ_λ is the spectral reflectivity). The emittance (ε) can be calculated using the formula

$$\varepsilon = \frac{\int_{\lambda_1}^{\lambda_2} (1-\rho_\lambda) E_{b\lambda}(T)\,d\lambda}{\int_{\lambda_1}^{\lambda_2} E_{b\lambda}(T)\,d\lambda} \tag{2}$$

Where $E_{b\lambda}$ (T) denotes the blackbody radiation at temperature T.

2　Results and discussion

CNTs possess excellent electrical conductivity[22], which could reduce the resistivity of the plating bath. Conventional black nickel could not be prepared with the current density of composite electrodeposition. The SEM image (Fig. 2(a)) recorded on S-3400 (Hitachi, Japan) reveals that the structure of conventional black nickel is dense, which the current density of preparing is 0.15 A/dm^2. Fig. 2(b) refers to the SEM image of black nickel prepared with current density of composite electrodeposition (0.5 A/dm^2), showing abnormal growth of crystalline grain and colour of the coating compared with Fig. 2(a). Under high

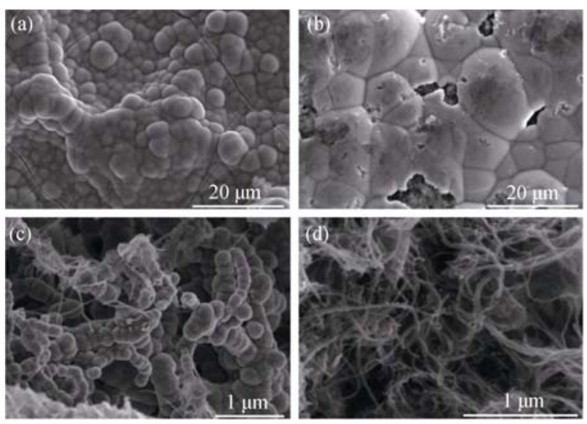

Fig. 2　(a) SEM image of conventional black nickel (current density is 0.15 A/dm^2), (b) SEM image of black nickel (current density is 0.5 A/dm^2) and (c, d) SEM images of composite coating (current density is 0.5 A/dm^2)

magnification, the SEM images (Fig. 2(c) and(d)) of CNTs/black nickel composite coating measured with SU8820 (Hitachi, Japan) indicate that compared with conventional black nickel coating, grain size of composite coating is smaller, and microporous structure has been formed. Fig. 2(d) refers to the partial of composite coating, showing that there are twisting CNTs in the composite coating. The CNTs covering on the surface of cathodes provided more nucleation sites, which hindered the growth of crystal nucleus. There is a competition between the nucleation and growth of crystals. Furthermore, too many nucleation sites suppressed the growth of crystal nucleus, which lead to the decrease of grain size of the composite coating. Some of CNTs surfaces were covered with grains, which indicates that metal ions were not randomly deposited on the surface of CNTs. Metal ions preferentially reduce on defects of the surface or both ends of CNTs where activities of atoms were large, while nucleation energy was small. The isotropic of crystal growth gave rise to black nickel with pearl serial structure during the process of electrodeposition. This phenomenon results in the microporous structure of composite coating. Due to uncompleted dispersion, some CNTs formed small aggregates. These small aggregates were covered up by coating, which lead to the uneven surface and increase of roughness of composite coating.

The cross section of composite coating was observed. According to the SEM result (Fig. 3(a) and 3(b)), it shows the thickness (marked with white arrow) of composite coating with electrodeposition treatment for 30 min and 60 min which was about 30 μm and 60 μm, respectively. By contrast, it was much thicker than that of conventional black nickel coating for 2–3 μm. With the addition of CNTs in the electrolyte, it could decrease the electrical resistivity, which increased the rate of deposition. With that, the thickness of composite coating could be increased. Moreover, CNTs combined with coatings caused point discharge effect, which could accelerate the deposition of metal ions as well as increase the thickness of composite coating. Fig. 3(c), which is under high magnification of Fig. 3(b), reveals that the structure is not dense and there are multiple pores in the composite coating, which is beneficial to increase the absorption of light.

The experiment measured solar absorptance and IR emittance of the composite coating as well as conventional black nickel coating. The conventional black nickel coating prepared by the same electrolyte, bath temperature, the pH value and deposition time were applied in composite coating. The preparation method of coatings is the same except current density. Fig. 4(a) shows the spectral reflectance of two coatings in the spectra range of 300–2300 nm. The solar absorptance of conventional black nickel coating is 94% calculated by Eq. (1), yet the solar absorptance of composite coating is 98%. Fig. 4(b) plots the infrared spectral reflectance in the wavelength range of 2.5–20 μm of conventional black nickel coating and composite coating. The

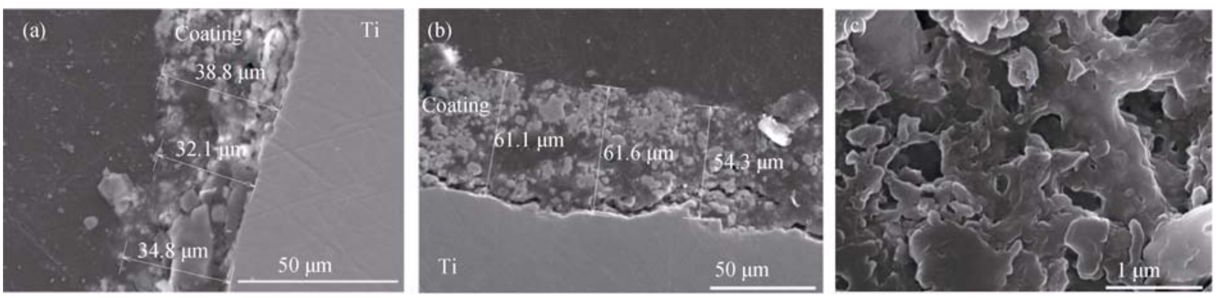

Fig. 3 Cross section images of composite coating with electrodeposition for 30 min and 60 min (a, b, c)

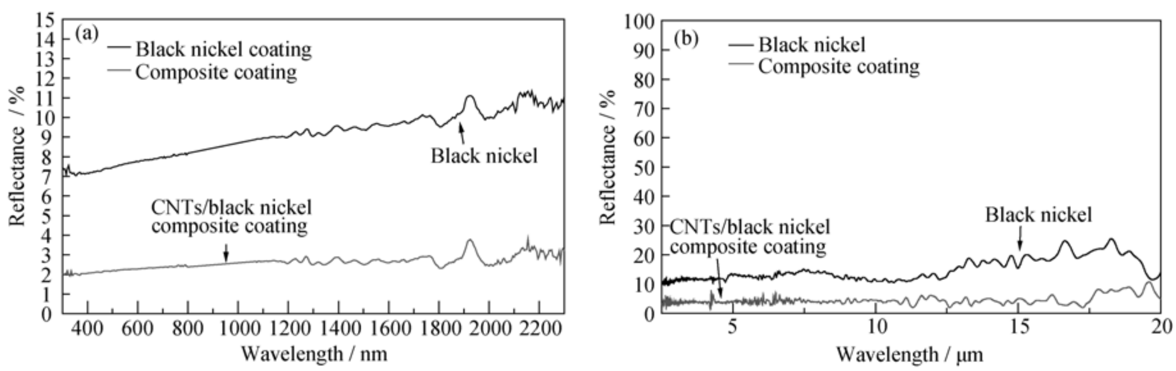

Fig. 4 (a) Reflection spectra and (b) IR spectral reflectance of composite coatings calculation results obtained by Eq. (2)indicate that the CNTs dramatically improved optical properties of black nickel. Indeed, CNTs has a high absorption coefficient[14] and capability to absorb incident light. Furthermore, the pore structures in the composite coatings act as traps for light absorption. Multiple reflections occur when light comes into these pores. Also, gaps between the non-fully dispersed CNTs (Fig. 2(d)) can act as light traps. The small aggregates of CNTs formed a sparse structure which could suppress the reflection. The pore diameter, pore depth, and spacing of light traps are different. Dimensions of these traps are comparable to the wavelength of incident lights. In consequence, composite coating can absorb lights in wide spectral range. Additionally, the decrease of grain size and the increase of surface roughness are the factors for improving optical properties.

The influence of CNTs concentration in the range of 0–1.5 g/L on the optical properties of composite coating was investigated. The results are shown in Fig. 5(a). The solar absorptance increases firstly, then decays, as concentration of CNTs increasing. Low CNTs concentration in the electrolyte results that CNTs are hard to co-deposit with black nickel to form composite coating. While high concentration leads to increase of aggregation of CNTs, which may cause the heterogeneity of coating. The concentration of 1.0 g/L of CNTs can achieve the highest solar absorptance. The influence of current density of electrodeposition in the range of 0.2–0.6 A/dm^2 on the solar absorptance of composite coating was presented in Fig. 5(b). High current density leads to increase deposition rate, which contributes to co-deposition of CNTs and black nickel to form the composite coating. Excessive current density results that the reduction rate of black nickel is so fast that CNTs can't diffuse to the surface of electrode. Thus, the composite coating is hard to be formed. The optimum result was obtained at current density of 0.5 A/dm^2.

3 Conclusions

CNTs/black nickel composite coating was successfully fabricated by using electrochemical deposition method. The microstructure of coating was changed by introduc ing CNTs into black nickel coating and the optical properties of composite coating were dramatically improved. The composite coating is capable with the result of small grain size of microporous coating. In addition, the roughness of composite coating increased, of absorbing 98% light in solar region (300–2300 nm), while the emittance over 2.5–20 μm range was 94%, better than those of conventional black nickel coatings. Those findings suggest that the CNTs/black nickel composite coating by electrodeposition method may provide a new route for light absorption materials fabrication with advanced optical properties.

References:

[1] SMITH S M. Specular reflectance of optical-black coatings in the far infrared. *Applied Optics*, 1984, **23(14):** 2311–2326.

[2] HAGOPIAN J G, GETTY S A, QUIJADA M, *et al*. Multiwalled Carbon Nanotubes for Stray Light Suppression in Space Flight Instruments. Carbon Nanotubes, Graphene, and Associated Devices III. San Diego, 2010, 77610.

[3] KODAMA S, HORIUCHI M, KUNII T, *et al*. Ultra-black nickel-phsdphorus alloy optical absorber. *IEEE. Transactions on Instrumentation and Measurement*, 1990, **39(1):** 230–232.

[4] RANI R U, SHARMA A K, MINU C, *et al*. Studies on black electroless nickel coatings on titanium alloys for spacecraft thermal control applications. *Journal of Applied Electrochemistry*, 2010, **40(2):** 333–339.

[5] XING F, ZHAO B, SHI W. Study on tunable fabrication of the ultra-black Ni–P film and its blacking mechanism. *Electrochimica Acta*, 2013, **100:** 157–163.

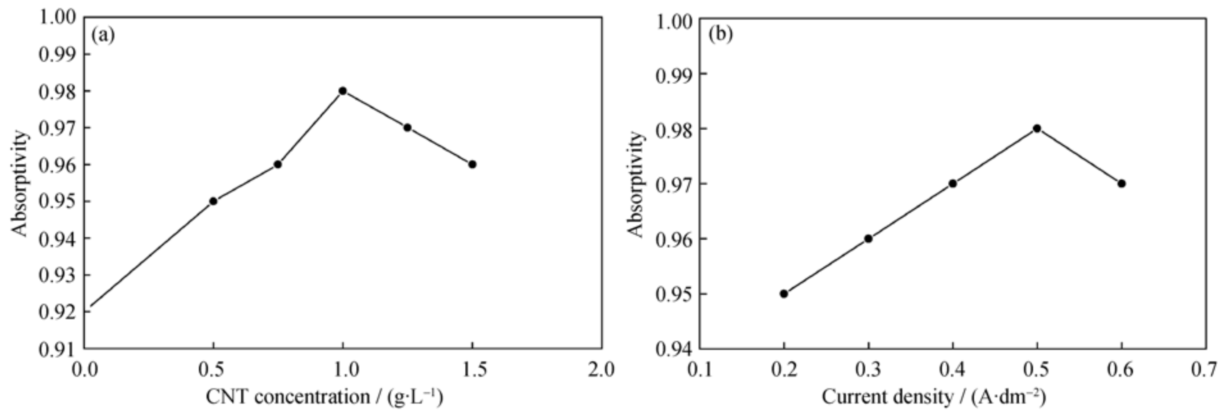

Fig. 5　Effect of CNT concentration (a) and current density on absorptance (b)

[6] LIRA-CANTÚ M, MORALES SABIO A, BRUSTENGA A, *et al*. Electrochemical deposition of black nickel solar absorber coatings on stainless steel AISI316L for thermal solar cells. *Solar Energy Materials and Solar Cells*, 2005, **87(1-4):** 685–694.

[7] MELLOUKI I, BENNAJI N, YACOUBI N. IR characterization of graphite black-coating for cryogenic detectors. *Infrared Physics & Technology*, 2007, **50(1):** 58–62.

[8] WACKELGARD E. Characterization of black nickel solar absorber coatings electroplated in a nickel chlorine aqueous solution. *Solar Energy Materials and Solar Cells*, 1998, **56(1):** 35–44.

[9] IBRAHIM M A M. Black nickel electrodeposition from a modified Watts bath. *Journal of Applied Electrochemistry*, 2005, **36(3):** 295–301.

[10] MIZUNO K, ISHII J, KISHIDA H, *et al*. A black body absorberfrom vertically aligned single-walled carbon nanotubes. *Proceedings of the National Academy of Sciences*, 2009, **106(15):** 6044–6047.

[11] IIJIMA S. Helical microtubules of graphitic carbon. *Nature*, 1991, **354(6348):** 56–58.

[12] AURISICCHIO C, MAREGA R, CORVAGLIA V, *et al*. CNTs in optoelectronic devices: new structural and photophysical insights on porphyrin-DWCNTs hybrid materials. *Advanced Functional Materials*, 2012, **22(15):** 3209–3222.

[13] YANG N, XU X, ZHANG G, *et al*. Thermal transport in nanostructures. *AIP Advances*, 2012, **2(4):** 041410.

[14] YANG L, WANG S, ZENG Q, *et al*. Carbon nanotube photoelectronic and photovoltaic devices and their applications in infrared detection. *Small*, 2013, **9(8):** 1225–1236.

[15] KAUL A B, COLES J B, EASTWOOD M, *et al*. Ultra-high optical absorption efficiency from the ultraviolet to the infrared using multi-walled carbon nanotube ensembles. *Small*, 2013, **9(7):** 1058–1065.

[16] WANG X J, FLICKER J D, LEE B J, *et al*. Visible and near-infrared radiative properties of vertically aligned multi-walled carbon nanotubes. *Nanotechnology*, 2009, **20(21):** 215704.

[17] SHI H, OK J G, BAAC H W, *et al*. Low density carbon nanotube forest as an index-matched and near perfect absorption coating. *Applied Physics Letters*, 2011, **99(21):** 211103.

[18] YANG Z P, CI L, BUR J A, *et al*. Experimental observation of an extremely dark material made by a low-density nanotube array. *Nano Letters*, 2008, **8(2):** 446–451.

[19] RODRIGUES J, MATA D, PIMENTEL A, *et al*. One-step synthesis of ZnO decorated CNT buckypaper composites and their optical and electrical properties. *Materials Science and Engineering B-Advanced Functional Solid-State Materials*, 2015, **195(1):** 38–44.

[20] CHEN X H, CHEN C S, XIAO H N, *et al*. Corrosion behavior of carbon nanotubes-Ni composite coating. *Surface & Coatings Technology*, 2005, **191(2/3):** 351–356.

[21] CHEN Z, BOSTROM T. Electrophoretically deposited carbon nanotube spectrally selective solar absorbers. *Solar Energy Materials and Solar Cells*, 2016, **144:** 678–683.

[22] XIE X L, MAI Y W, ZHOU X P. Dispersion and alignment of carbon nanotubes in polymer matrix: a review. *Materials Science and Engineering: R: Reports*, 2005, **49(4):** 89–112.

电沉积法制备碳纳米管/黑镍复合涂层的光学与结构特性

邹斯浩, 辛世刚, 宋力昕

(中国科学院 上海硅酸盐研究所, 特种无机涂层重点实验室, 上海 200050)

摘 要: 利用复合电沉积的方法在钛合金基体上成功制备出具有优异光学性能的碳纳米管 / 黑镍复合涂层, 并研究了复合涂层的微观形貌、光学性能以及镀液中碳纳米管浓度和电镀电流密度对光学性能的影响。实验结果表明: 相较于传统电镀方法获得的单一黑镍涂层, 复合涂层的晶粒尺寸明显减小, 形成多孔结构, 表面粗糙程度明显增加。复合涂层对 300~2300 nm 范围内的入射光吸收率达到 98%左右, 在 2.5~20 μm 范围内的红外吸收率达到 94%, 远远高于传统单一黑镍涂层。复合涂层的太阳吸收比会随着镀液中碳纳米管浓度与电镀电流密度的增加呈先增大后减小的变化规律。

关 键 词: 碳纳米管; 电沉积; 复合涂层; 太阳吸收比

中图分类号: TQ174 **文献标识码:** A